Send Orders for Reprints to reprints@benthamscience.ae

Protein & Peptide Letters, 2015, *22*, 000-000

Assessment of a Protease Inhibitor Peptide for Anti-Ageing

Madalena Martins[†], Nuno G. Azoia[†], Ana C. Carvalho[‡], Carla Silva[†§], Teresa Matamá[†‡], Andreia C. Gomes[‡] and Artur Cavaco-Paulo[†*]

[†]*Centre of Biological Engineering (CEB), University of Minho, Campus of Gualtar, 4710-057 Braga, Portugal;* [‡]*Molecular and Environmental Biology Centre (CBMA), Department of Biology, University of Minho, Campus of Gualtar, 4710-057 Braga, Portugal;* [§]*Present address: 3B's: Biomaterials, Biodegradables and Biomimetics, Dept. of Polymer Engineering, University of Minho, AvePark, Zona Industrial da Gandra, S. Cláudio do Barco, 4806-909 Caldas das Taipas, Guimarães, Portugal*

Artur Cavaco-Paulo

Abstract: Ageing and skin exposure to UV radiation induces production and activation of matrix metalloproteinases (MMPs) and human neutrophil elastase (HNE). These enzymes are known to break down the extracellular matrix (ECM) which leads to wrinkle formation. Here, we demonstrated the potential of a solid-in-oil nanodispersion containing a competitive inhibitor peptide of HNE mixed with hyaluronic acid (HA), displaying 158 nm of mean diameter, to protect the skin against the ageing effects. Western blot analysis demonstrated that activation of MMP-1 in fibroblasts by HNE treatment is inhibited by the solid-in-oil nanodispersion containing the peptide and HA. The results clearly demonstrate that solid-in-oil nanodispersion containing the HNE inhibitor peptide is a promising strategy for anti-ageing effects. This effect can be seen particularly by ECM regulation by affecting fibroblasts. The formulation also enhances the formation of thicker bundles of actin filaments.

Keywords: Protease, inhibitory peptide, proteolysis, immunoassay, diffusion, nanodispersion.

INTRODUCTION

The ageing effects of exposure to sunlight on human skin have been largely recognized. The alterations provoked in skin are mostly caused by ultraviolet spectrum (wavelengths between 240-400 nm). Extended and continuum exposure to ultraviolet radiation (UV) will accelerate skin aging, typically designated as photoaging [1]. The severity of photoaging depends on cumulative sun exposure, occupation and life-style [2]. It is characterized by the appearance of wrinkles, laxity, roughness, dryness and irregular pigmentation [3]. It has also been reported that photoaging is associated with the increased of collagenase synthesis resulting in a thinned epidermis, dysplasia of keratinocyte and collagen degradation in the layers of the dermis. The decrement of collagen production is related with the loses of elasticity, and the breakdown of fibroblasts are related with the wrinkles formation [4].

The extracellular matrix (ECM) is composed by the most common components secreted by fibroblasts like viscous proteoglycans, fibronectin and collagen fibers [5]. Elastase type-proteases are shown to actively degrade fibronectin [6]. Elastase is the major product from activated skin-infiltrating neutrophils that expand the inflammatory response initiated by UV radiation. Biologically, the breakdown of elastin and collagen as well as the augment of elastase activity promotes the decline of elasticity and the subsequent formation of the stretchmarks and wrinkles [7]. Human neutrophil elastase (HNE) is an enzyme capable of degrading almost all ECM proteins as well as a variety of key plasma proteins [8].

Matrix metalloproteinase (MMPs) is a family of extracellular zinc-containing endopeptidases [5a, 5c, 5d, 9]. The ECM is composed by their substrates which are different types of collagen, matrix glycoproteins and proteoglycans. MMPs are grouped through substrate specificities as membrane-type MMPs, stromelysins, gelatinases and collagenases. MMPs strongly contribute to the ECM damage and the decreased procollagen synthesis leading to the formation of photoaged skin [10]. In addition, the damage of the dermal ECM is histologically characterized by the accumulation of disintegrated abnormal elastic fibers in the upper dermis [11]. The identification of products capable to inhibit MMPs is emerging in pharmaceutical area for the prevention or aging treatment of skin [12].

The harmful effects on skin from UVs radiation can be direct and indirectly formed. After chronic UV irradiation, neutrophils infiltrate into the skin and release HNE, which participates both direct and indirectly in the formation of wrinkles. HNE is indirectly involved in ECM deterioration by the activation of matrix MMPs and through direct proteolytic action [13]. Therefore, the inhibition of elastase activity and the subsequent inhibition of active MMPs might be an effective method to protect and/or prevent skin aging effects.

Herein, we used a methodology of solid-in-oil nanodispersion containing a HNE inhibitory peptide, which could be potentially applied for anti-ageing effects. We described re-

*Address correspondence to this author at the Centre of Biological Engineering, University of Minho, 4710-057 Braga, Portugal; Tel: +351 253 604 400; Fax: +351 253 604 429; E-mail: artur@deb.uminho.pt

0929-8665/15 $58.00+.00

cently a solid-in-oil nanodispersion technique for transdermally delivery large hydrophilic macromolecules like bovine serum albumin (BSA) and hyaluronic acid [14]. Here, we access the anti-ageing effects of a peptide after perfusion through the skin. The strongest HNE inhibitory peptide was chosen based on the HNE inhibitory activity of two peptides (with the Bowman–Birk reactive-site loop motive) studied for wound healing applications [15]. Western blot analyses were performed to demonstrate its capacity to prevent the activation of MMP1 by HNE *in vitro*. In addition, actin filaments of the cytoskeleton of human skin fibroblasts were evaluated by staining with phalloidin. This solid-in-oil nanodispersion is a promising strategy for the development of a new cosmetic product for ECM homeostasis, preventing its degradation by inhibition of MMP-1 and dermal fibroblasts increased cytoskeleton density.

MATERIALS AND METHODS

Materials

The peptide ((MGWCTASVPPQCY$(GA)_7$, 2339.62 g/mol) was synthetized by JPT Peptide Tecnologies GmbH (Germany). Sucrose ester (SE) was purchased from Sisterna (Netherland). Hyaluronic acid ($20 \leq Mw \leq 50$ kDa) was kindly provided from Soliance (France). Regarding histological preparations, the Immuno-Mount compound was acquired from Fisher Healthcare (UK) and the cryoprotectant compound was purchased from Sakura (Netherland). The SDS-PAGE and Western Blotting solutions were purchased to BioRad (Portugal). All other chemical and biochemical reagents were analytical grade and purchased from Sigma-Aldrich (USA).

The percutaneous studies were accomplished by pig skin kindly provided by the slaughterhouse Matadouro Central de Entre Douro e Minho (Portugal). The cell line (hTERT) BJ5ta, an immortalized human dermal fibroblasts, was acquired by European Collection of Cells Culture (ECACC) and cultured following the recommendations of ATCC. The ASF-2 cells (human skin fibroblasts) were isolated and maintained as described by Cristovão *et al*. [16]. The human keratinocyte cell line, NCTC 2544, was obtained from Instituto Zooprofilattico Sperimentale della Lombardia e dell'Emilia Romagna (Brescia, Italy) and maintained according to the supplier instructions.

Assessment of Indirect Inhibitory Activity of the Peptide on MMP-1 Proteolytic Activation *In Vitro* by Western Blot

To determine the ability of the formulation to prevent pro-MMP1 activation, the chosen concentration was based on the lowest dilution without cytotoxicity. The concentration used was 2% (v/v) of peptide/HA solid-in-oil nanodispersion, corresponding to 10 μg of peptide for each mL of culture medium. The BJ5ta fibroblasts were grown in DMEM (Dulbecco's Modified Eagle's Medium) with 10% FBS, seeded at 155000 cells in a 12-well cell plates. The replacement of culture medium (with DMEM) was performed after 24 hours post-seeding followed by the addition of 1 ng/mL of TNF-α for 48h, to induce the metalloproteinase proMMP-1. Then, for the proteolytic activation of the proMMP-1, HNE was added 24h before the end of the 48h incubation period (20 mU of HNE, Sigma). Thirty minutes after adding the HNE, the inhibitors, the same amount of free peptide and formulated peptide, were added to the wells. When the experiment ended, the culture media it was taken and concentrated by lyophilization.

After rehydration, the total amount of protein was determined by DC Assay (colorimetric assay for protein concentration, BioRad). The samples were diluted to normalize the values to the least concentrated sample (around 0.72 μg/μL) and the maximum volume was loaded (20 μL) and the culture media samples were analyzed by 12% SDS-PAGE. The gel was then transferred onto a polyvinylidine difluoride (PVDF) membrane (BioRad). The membrane was blocked with blocking buffer for one hour and then it was incubated with purified antibody (polyclonal rabbit) against the N-terminus of human MMP-1 (Sc-8834-R, Santa Cruz Biotechnology, Germany) for 2 h. After that, the membrane was washed and was proceeded to its incubation with HRP-labeled goat anti-rabbit IgG (sc-2004, Santa Cruz Biotechnology, Germany) with 1 μL of the HRP conjugate (Precision protein Strep Tactin- BioRad, Portugal) for one hour. The membrane was rinsed and then incubated using the mix substrate kit components (ECL Clarity, BioRad) in a 1:1 ratio for 5 min. Bands detected on the PVDF membrane were analyzed by chemiluminescence (Chemidoc XRS + System, BioRad, Portugal).

Effect of the Formulated HA on the Cytoskeleton of Fibroblasts by Fluorescent Phalloidin

Two types of fibroblasts (immortalized fibroblasts: BJ-5ta cell line and primary human fibroblasts: ASF-2) were cultured for 24 hours at low confluence (50000 cells per well). The cells were grown on sterile coverslips in the bottom of each 24-well cell plates of polystyrene, in the presence or absence of hyaluronic acid, either formulated or in the free form. After washing three times with PBS at 37ºC, cells were fixed at room temperature using 3.7% of formaldehyde in PBS during 10 minutes. Then, cells were washed two times with PBS. Thereafter, cells were permeabilized in 0.1% of Triton X-100 (in PBS) for 3-5 minutes and then were washed two times with PBS. The cytoskeleton was stained with 5 U/mL phalloidin incubated for 20 minutes at room temperature in the dark. Once washed with PBS, the coverslip was removed from the well with forceps and the excess of PBS was allowed to drip off. Coverslips were mounted (cells facing down) onto the slide containing one drop of anti-fade mounting medium (Vectashield® Mounting Media). This medium is glycerol-based and it contains the counterstain 4', 6-diamidino-2-phenylindole (DAPI) that, when bound to DNA produces a blue fluorescence. Slides were analyzed under Olympus IX70 inverted epi-fluorescence microscope, using Cell^F Imaging Solutions GmbH software (v3.4). The cell morphology and cytoskeleton effect (actin filaments density) were analyzed.

Percutaneous Studies: Qualitative and Quantitative Penetration Profile

The skin specimens were prepared by carefully removing the subcutaneous fat, and then immediately used for penetra-

tion studies. *In vitro* penetration studies were performed using a Franz diffusion cell (PermeGear, USA). The skin samples were sandwiched between the upper (donor chamber) and bottom (receptor chamber) compartment. In the donor chamber was placed 300 µL of the formulation and in the receptor chamber was placed 5 mL of PBS (phosphate-buffered saline, 0.01 M, pH 7.4) which was maintained at 37ºC, so the skin sample reaches 32±1 ºC, the physiological skin temperature, in a circulating water bath (Thermo Scientific SC 100, Germany). An aliquot (150 µl) of the receptor compartment was collected at predetermined time intervals, 0, 2, 4, 6, 8, 24, 48 and 72 hours. Fresh buffer was replaced for each volume removed. The percutaneous penetration was assessed using the Lowry assay to quantify the protein concentration and monitoring the absorbance at 185 nm to detect the HA concentration for each sample removed. Controls samples, without the presence of peptide and HA, were performed.

The qualitative permeation profile of peptide/HA solid-in-oil nanodispersion through the skin was performed by confocal laser scanning microscopy. In order to profile the permeation, a solid-in-oil nanodispersion was prepared with the Fluorescein Isocyanate (FITC)- labelled peptide and the Rhodamine Isocyanate (RITC)- labelled HA. After 72 hours, the removal pig skin specimens from Franz cells were performed. Then, these skin samples were incorporated into OCT and frozen at -80ºC. The frozen skin samples were sectioned with a cryostat into 20 µm slices. The permeation of the fluorescent compounds was assessed by confocal laser microscopy (Leica TCS SPE, Germany). All optical sections were recorded with the same settings. The slides of FITC-labelled peptide which fluorescent emission signal is represented by a green colour. RITC labelled HA which fluorescent emission signal is represented by a red colour.

Molecular Dynamics Simulation

For the simulations we used the software package GROMACS [17] (version 4.6.2). The force filed used was Martini [18]. The size of the simulation box was determined according to the minimum image convention (according to a cut-off of 1.2 nm). LINCS [19] was used to constrain the bonds lengths and the non-bonded interactions were calculated using a twin-range method (short range cut-off = 0.9 nm, long range cut-off = 1.2 nm). Neighbour search was updated every ten steps and carried out up to 1.2 nm. The integration time step used was 5 fs, and for the electrostatics interactions we considered a reaction field correction using a dielectric constant of 15. Berendsen barostat [20] and Berendsen thermostat [20] were used. Reference pressure of 1 bar, 3.0 ps of relaxation time and isothermal compressibility of 3.0×10^{-5} bar^{-1}. Temperature was set at 300 K. Separated heat baths (coupling constants of 0.30 ps) were considered for each component of the system. Two replica simulations (320 ns in length) were carried out. Different initial velocities were taken from a Maxwell-Boltzman distribution at 300 K. The lipid membrane and the proteic nanoemulsion were built using the same approach described in our previous work [14b].

RESULTS

In Vitro Inhibitory Activity of the Peptide/HA Nanoformulation on Ageing-Associated Proteases by Western Blot

In vitro detection by western blot demonstrated a decreased level of active MMP-1 due to the HNE inhibition, where it was dependent on the availability of the peptide to the dermal fibroblasts (Fig. **1**). The control formulation using BSA instead of the peptide was not able to inhibit HNE (data not shown).

Considering that cytokines can induce the production of MMPs by fibroblasts, we stimulated fibroblasts with TNF-α. When fibroblasts were stimulated by adding to the medium the cytokine TNF-α, the induction of proMMP-1 (Mw 54 kDa) was observed after 48h (Fig.1: lane 2-5), compared to the basal levels secreted by fibroblasts without TNF-α (Fig.1: lane 1). MMP-1 is secreted by fibroblasts in its inactive form (proMMP-1) being activated when cleaved by HNE released by Neutrophil cells recruited after a stimuli like UV radiation [13]. Thus, we incubated the fibroblasts with 20 mU/mL HNE 24 hours after addition of TNF-α (HNE concentration was non-toxic data not shown). After 30 minutes of exposure to HNE, the inhibitors (free and formulated peptide) were added to the medium. As shown in Fig.1, MMP-1 was not activated in the absence of HNE (lane 2), only being activated in the presence of HNE (lane 3-5: peptides at 22/25 and 27 kDa).

Assessment of Actin Cytoskeleton by Dermal Fibroblasts in Contact with Peptide/HA Nanoformulation

The assessment of actin cytoskeleton display vital impact in cell`s mechanical **stability** and the evaluation of actin fibers it is essential to demonstrate anti-ageing benefits. The effect of HA on the cytoskeleton of dermal fibroblasts was evaluated in two types of cells: immortalized human normal skin fibroblasts (BJ-5ta) and primary human fibroblasts (ASF-2). After exposing fibroblasts for 24 hours in presence or absence of HA in formulated and free form, the actin filaments density was analyzed through inverted epi-fluorescent microscope. The images in Fig. **2** shows that the presence of HA contributes for a dense actin filament bundles for both cell types.. This assessment was revealed by staining with fluorescently labelled phalloidin.

Qualitative and Quantitative Percutaneous Profile

The perfusion of peptide/HA into the skin was successfully achieved using the S/O nanodispersion. Fig. **3** clearly demonstrates that the S/O nanodispersion of peptide/HA crosses the *stratum corneum* (SC) barrier spreading into epidermis and dermis of the skin. The images reveal the effective permeation of the peptide labelled with FITC (green) and hyaluronic acid labeled with RITC (red) into the different layers of pig skin.

The skin permeability of peptide/HA was also examined quantitatively (according to our preceding study) [14a]. Considering the cumulative amount of peptide and HA, the effective penetration of peptide/HA S/O nanodispersion through the skin was shown in Table **1**.

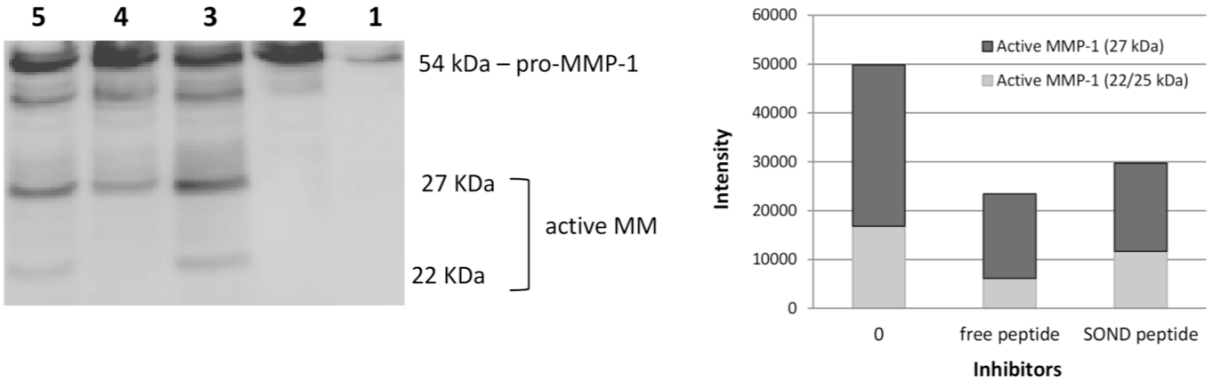

Figure 1. Inhibition of active MMP-1 secreted by fibroblasts when cleaved by HNE was assayed by analysis of western blot. Lane 1 and 2: 0 and 1 ng/mL of TNF-α, respectively; Lane 3: 1 ng/mL of TNF-α plus 20 mU/mL of HNE; Lane 4: 1 ng/mL of TNF-α with 20 mU/mL of HNE plus free peptide and lane 5 equal to lane 4 but with peptide/HA solid-in-oil nanodispersion (SOND). In order to confirm the intensity of each band was quantified using integrated density by Image J software.

(A)

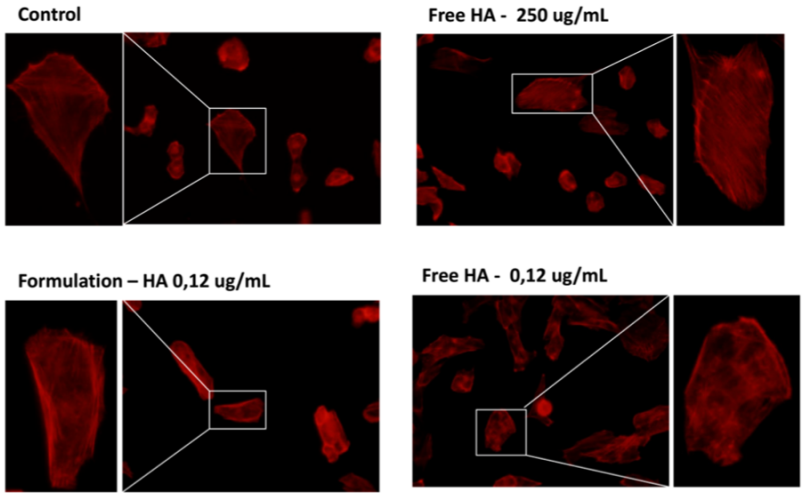

(B)

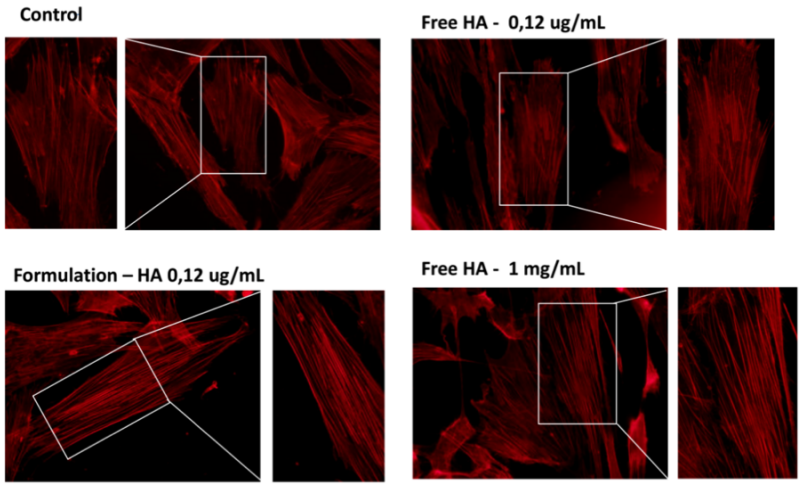

Figure 2. Images of actin cytoskeleton of dermal fibroblasts (A) BJ-5ta immortalized fibroblasts and (B) ASF-2 normal human fibroblasts revealed by fluorescent phalloidin. Cells grown at different conditions: control, formulated HA into peptide/HA solid-in-oil nanodispersion (0.12 µg/mL), free HA (0.12 µg/mL) and positive control (free HA 1mg/mL), in the culture medium from 24 hours.

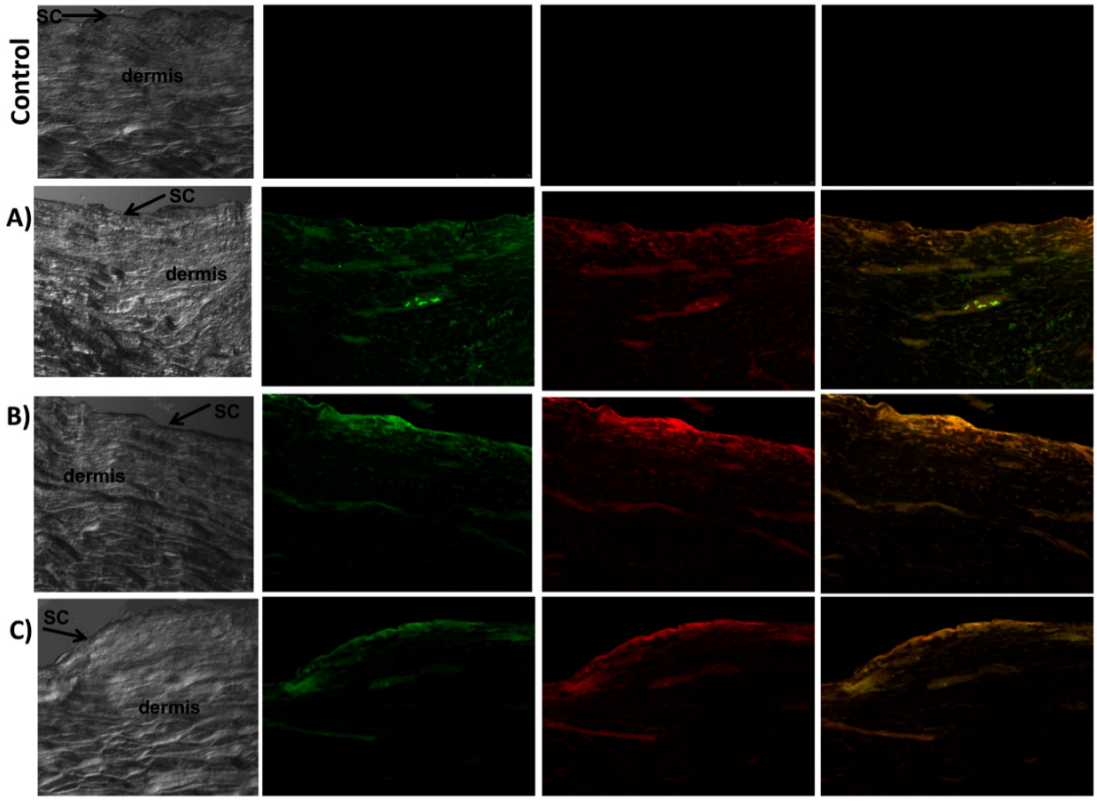

Figure 3. Confocal 2D images of pig skin crossed by peptide/HA solid-in-oil nanodispersion. Images of control sample, formulation non-diluted (A), formulation at 2% (v/v) (B) and 0.5% (v/v) (C). Figure shows the phase contrast images, FITC pictures (green colour with maximum emission at 520 nm) emitting FITC-labelled peptide and RITC (red colour with maximum emission at 595nm) emitting RITC-labeled HA. The Merge pictures combine FITC and RITC signals.

Table 1. Cumulative amount of peptide/HA solid-in-oil nanodispersion 2% (v/v) permeated after 0.5, 2, 8, 24 and 48 hours through pig skin (surface area 0.785 cm^2) maintained at 37ºC. Each value represents the mean cumulative amount for 3 experiments ± standard deviation.

Time of permeation (hours)	Cumulative amount (Qt) (µg/cm^2)
0.5	52.3 ± 3.9
2	156.7 ± 4.2
8	230.9 ± 5.4
24	271.5 ± 4.5
48	338.8 ± 3.9

Molecular dynamics simulations predicted and confirmed skin permeation of this formulation (Fig. **4**). The image demonstrates that the peptide/HA S/O nanodispersion after 300 ns is completely integrated into the top bilayer.

The nanodispersion formulation was fundamental to transdermally delivery hydrophilic components through the skin. The combination of the peptide and HA spread into the skin constitute a great strategy for possible cosmetics applications, especially related with anti-ageing (Fig. **5**).

DISCUSSION

In this paper, we access the anti-ageing effects of a peptide after it perfusion through the skin. The peptide (competitive inhibitor for HNE) was delivered across the skin using a solid-in-oil nanodispersion with HA. The production yield (calculated according other previous study [14a]) of the formulation was around 78%. Previous studies performed by Vasconcelos *et. al.*, 2011, demonstrated that this peptide is a competitive inhibitor for HNE [15]. This short peptide sequence has the potential to be incorporated in skin anti-ageing formulations based on its capacity to inhibit ageing-associated proteases (HNE and indirectly MMP-1) of ECM produced by dermal fibroblasts.

The skin ageing process is divided into two categories, intrinsic ageing and extrinsic ageing (known as photoaging) [21]. The first category is identified by dried, smooth, pallid and fine wrinkled skin aspect; the second category is identified by alterations of pigmentation and formation of wrinkles, typically in the face and neck as well as forearm which are the areas typically exposed to the sun [8]. Several evidences established a strong correlation between the formation of wrinkles and the MMPS actions [22]. Researchers have been assuming that dermal connective tissue can suffer alterations in skin areas exposed to radiation from the sun

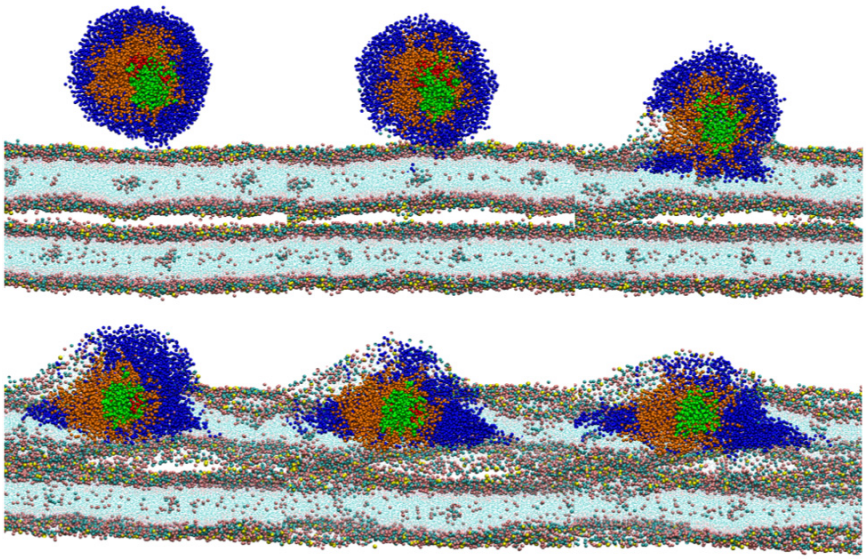

Figure 4. Representation of time evolution by computational dynamics simulation. The picture illustrates snapshots of the dynamics simulations at 0 ns, 60 ns, 120 ns, 180 ns, 240 ns and 300 ns. The peptide is represented by green color, hyaluronic acid by red, Surfactant SE by orange and IPM by blue color.

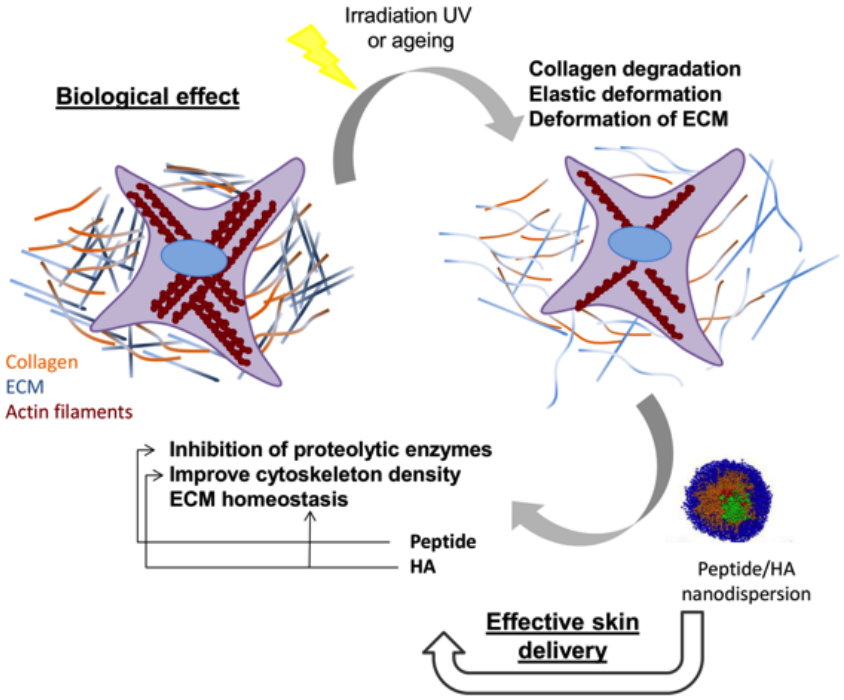

Figure 5. Schematic representation of the methodology used and biology effects of the peptide and HA after perfusion through the skin.

[13, 23]. It is believed that UVs radiation, particularly UVB, plays an important role in photoaging process and induces the expression of MMP-1 (interstitial collagenase of MMPs) in human dermal and epidermis layers [24].

Herein, in order to examine the inhibition of MMP-1 secreted by fibroblasts from peptide/HA solid-in-oil nanodispersion, activation of MMP-1 in fibroblasts was required. The amount of TNF-α and time for the MMP1 induction in BJ5ta was optimized and the peptide/HA nanodispersion was not able *per si* to induce MMP-1 induction (data not shown).

In Fig. **1** the results strongly indicate that the peptide is able to lower the amount of active MMP1 by inhibiting the proteolytic activity of HNE (lane 4 and 5). Protein bands did not show signal saturation. It is also worth of note that the free peptide presents a stronger inhibitory effect (lane 4) than the formulated peptide (lane 5) which demonstrate that when

all formulation crosses the skin the peptide dissociates from the nanodispersion being completely free to act. Once MMP-1 plays greater role in maintaining elasticity of the skin and it resilience, to prevent or inhibit MMP-1 action constitute a potential approach to reduce or prevent photoaging.

The data obtained from *ex vivo* permeation studies support the assumption that once this solid-in-oil nanodispersion penetrates the skin it has a strong tendency to dissociate due to various factors including the diffusion membrane material, skin conditions among others [14a]. Given that, once the peptide is disintegrated from the complex loses it spherical form becoming freely available to act into the skin. It is expected that this competitive HNE inhibitor peptide, MGWCT ASVPPQCYG$(GA)_7$, lower the levels of active MMP-1 and consequently be able to reduce subsequent collagen breakdown thereby preventing skin ageing. It is well documented that MMP-1 triggers the collagen degradation which unwinds the triple-helical collagen structure and break peptide bonds by hydrolysis [25]. After collagen degradation following its conversion to denaturated form, gelatin, and its degeneration by gelatinases [25]. Therefore, the inhibition of elastase and subsequently prevention or inhibition of active MMP-1 constitute pivotal role to reduce effects of skin ageing. Given that, these results suggest that the peptide/HA solid-in-oil nanodispersion could represent a valuable approach for the development of new cosmetic anti-ageing product.

Several outcomes in literature indicate that HA is a universal component of ECM and plays an important role in tissue hydration, cell function and ECM regulation [26]. Significant histological features of photoaged skin include the ECM deformation and collagen reduction. These characteristics lead to a loss of strength and elasticity of the skin. [27]. Once changes in mechanical properties could determine features of aged skin associated with degraded or degenerated elastic properties [28], it is essential to explore strategies to demonstrate anti-ageing benefits.

The interaction of the hyaluronic acid as a component of the ECM and cytoskeleton constituents is known to regulate important phenomena such as cell division and differentiation [29]. This is crucial for normal skin biology and preservation of its features including mechanical properties. Hence the presence of HA in peptide/HA solid-in-oil nanodispersion had an important effect on the density of cytoskeleton filaments. Cytoskeleton actin bundles encompass various vital cellular processes including the cytoskeleton stress fibers. Actin-based cytoskeleton bundles contribute to the actively regulated nuclear positioning during mitosis [30] and stabilize cell shape [31]. The proportion of actin expression is also correlated with the contractile efficiency of individual fibroblasts and hence with wrinkle formation [32]. The higher density of actin filaments suggests a possible modulation of fibroblasts cell stiffness, shape and migration which affect skin biology and ageing.

Fig. **2** presents the actin cytoskeleton comparing fibroblasts for both cell types (ASF-2 and BJ-5ta) for 24 hours. Our results point out those cells grown in the presence of HA exhibiting thicker actin filament bundles producing an actin cytoskeleton more prominent compared to controls. Peptide/HA formulation in the culture medium greatly enhanced the aggregation of actin which forms thick filament bundles. The presence of free HA also contributes for a dense actin filament bundles. This effect was effective for both types of cells being more pronounced for primary human fibroblasts (ASF-2). This result represents a great achievement once actin cytoskeleton plays greater role in the interaction between the ECM and fibroblasts. The combination of peptide with HA promotes an improvement in the density of cytoskeleton bundles that could constitute a valuable data to protect skin against ageing effects.

The perfusion profile of peptide/HA S/O nanodispersion into the skin was assessed qualitatively and quantitatively. Briefly, the solid-in-oil nanodispersion was prepared as follows: the mixture of peptide/HA was coated with a lipophilic surfactant and then highly dispersed in oil, generating spherical and homogeneous structures, as shown in supplementary data (Fig. S1 in Supplementary data). Storage stability was evaluated at room temperature, and the results indicated that peptide/HA solid-in-oil nanodispersion showed good stability over 2 months, presenting a slight aggregation after 3 months of storing (Fig. S2 in Supplementary data). No significant toxicity to the fibroblasts and keratinocytes was observed for formulation concentrations between 2.5 to 10 µg/mL of peptide and 0.03 to 0.12 µg/mL of HA, after 48h of incubation (Fig. S3 in Supplementary data).

From Fig. **3** the peptide/HA nanodispersion successfully permeated into the skin layers. The skin permeation was confirmed by molecular dynamics simulations (Fig. 4), showing that peptide/HA S/O nanodispersion was rapidly integrated into the lipids. The generated results obtained by the simulations demonstrated that each component of the formulations have it specific importance. Peptide/HA S/O nanodispersion are coated with hydrophobic surfactant molecules and then dispersed in IPM which plays greater role in S/O nanodispersion interaction with lipids. The formulation applied to the donor compartment, promotes high cumulative permeation amounts of peptide/HA through the skin (Table 1). The greatest permeation was observed at 48 hours indicating a great diffusion of the components. These results are fundamental to demonstrate a successful permeation of the peptide and hyaluronic acid spread into the skin. The overall of .nanodispersion methodology and the effects of each component, peptide and HA, after an effective skin delivery is crucial for their availability and biology performance (Fig. 5).

CONCLUSION

A potential cosmetic application for a competitive inhibitor peptide of HNE with HA was successfully established in this study. The formulation of the nanodispersion was fundamental to deliver the peptide and HA into the skin. The individual effect of each component, peptide that prevents or inhibits active MMP-1 and HA that preserves skin biology, showed remarkable advances for skin ageing.

The peptide/HA solid-in-oil nanodispersion successfully inhibit HNE action and therefore reduce the levels of active MMP-1 suggesting an indirect powerful anti-ageing benefit at the level of skin integrity and maintenance of elastic properties. Additionally, an enhancement in density of actin filaments bundles of dermal fibroblasts was achieved due to the presence of HA. These results obtained for an aqueous envi-

ronment of *in vitro* fibroblasts culture are reinforced by the good penetration profile into the deep layers of skin and dissociation of the nanodispersion complex. Thus, the results emphasize the huge prospective of peptide/HA soli-in-oil nanodispersion to be applied on a pharma/cosmetic composition products, specially designed for anti-ageing applications.

CONFLICT OF INTEREST

The authors confirm that this article content has no conflict of interest.

ACKNOWLEDGEMENTS

We thank Matadouro - Central Carnes de Entre Douro e Minho, Lda for their support on pig samples. The histological studies were supported by the Department of Histology from Life and Health Sciences Research Institute (ICVS), University of Minho. The authors thank the Fundação para a Ciência e Tecnologia the strategic funding of ID/BIO/04469/ 2013 unit.

SUPPLEMENTARY MATERIAL

Supplementary material is available on the publishers Web site along with the published article.

REFERENCES

[1] Cho, J. M.; Lee, Y. H.; Baek, R.-M.; Lee, S. W. *Journal of Plastic, Reconstructive & Aesthetic Surgery* 2011, *64* (2), e31-e39.

[2] Akiba, S.; Shinkura, R.; Miyamoto, K.; Hillebrand, G.; Yamaguchi, N.; Ichihashi, M. *J Epidemiol.* 1999, *9*, 136-142.

[3] Scharffetter–Kochanek, K.; Brenneisen, P.; Wenk, J.; Herrmann, G.; Ma, W.; Kuhr, L.; Meewes, C.; Wlaschek, M. *Exp. Gerontol.* 2000, *35* (3), 307-316.

[4] Fisher, G. J.; Varani, J.; Voorhees, J. J. *Arch. Dermatol.* 2008, *144*, 666-672.

[5] (a) Graham, H. K.; Horn, M.; Trafford, A. W. *Acta Physiologica* 2008, *194* (1), 3-21; (b) Porter, K. E.; Turner, N. A. *Pharmacology & Therapeutics* 2009, *123* (2), 255-278; (c) Spinale, F. *Physiol Rev.* 2007, *87* (4), 1285-342; (d) Spinale, F.; Coker, M.; Bond, B.; Zellner, J. *Cardiovasc Res.* 2000, *46* (2), 225-38.

[6] (a) McDonald, J. A.; Kelley, D. G. *J. Biol. Chem.* 1980, *255* (25), 8848-8858; (b) Labat-Robert, J.; Fourtanier, A.; Boyer-Lafargue, B.; Robert, L. *J. Photochem. Photobiol. B: Biol.* 2000, *57* (2–3), 113-118.

[7] Lee, K. K.; Kim, J. H.; Cho, J. J.; Choi, J. *Int. J. Cosmet. Sci.* 1999, *21* (2), 71-82.

[8] Havemann, K.; Gramse, M. *Adv. Exp. Med. Biol.* 1984, *167*, 1-20.

[9] Kukacka, J.; Průsa, R.; Kotaska, K.; Pelouch, V. *Biomed. Pap. Med. Fac. Univ. Palacky Olomouc Czech Repub.* 2005, *149* (2), 225-36.

[10] Shin, M. H.; Seo, J.-E.; Kim, Y. K.; Kim, K. H.; Chung, J. H. *Mech. Ageing Dev.* 2012, *133* (2–3), 92-98.

[11] (a) Muto, J.; Kuroda, K.; Wachi, H.; Hirose, S.; Tajima, S. *J. Invest. Dermatol.* 2006, *127* (6), 1358-1366; (b) Jung, S. K.; Lee, K. W.; Kim, H. Y.; Oh, M. H.; Byun, S.; Lim, S. H.; Heo, Y.-S.; Kang, N. J.; Bode, A. M.; Dong, Z.; Lee, H. J. *Biochem. Pharmacol.* 2010, *79* (10), 1455-1461; (c) Smith Jr, J. G.; Davidson, E. A.; Sams Jr, W. M.; Clark, R. D. *The Journal of Investigative Dermatology* 1962, *39* (4), 347-350.

[12] Philips, N.; Auler, S.; Hugo, R.; Gonzalez, S. *Enzyme Research* 2011, *2011*.

[13] Takeuchi, H.; Gomi, T.; Shishido, M.; Watanabe, H.; Suenobu, N. *J. Dermatol. Sci.* 2010, *60* (3), 151-158.

[14] (a) Martins, M.; Azoia, N. G.; Shimanovich, U.; Matamá, T.; Gomes, A. C.; Silva, C.; Cavaco-Paulo, A. *Mol. Pharm.* 2014, *11* (5), 1479-1488; (b) Martins, M.; Azoia, N. G.; Ribeiro, A.; Shimanovich, U.; Silva, C.; Cavaco-Paulo, A. *Colloids Surf. B. Biointerfaces* 2013, *108* (0), 271-278.

[15] Vasconcelos, A.; Azoia, N. G.; Carvalho, A. C.; Gomes, A. C.; Güebitz, G.; Cavaco-Paulo, A. *Eur. J. Pharmacol.* 2011, *666* (1–3), 53-60.

[16] Lima, C. F.; Pereira-Wilson, C.; Rattan, S. I. S. *Mol. Nutr. Food Res.* 2011, *55* (3), 430-442.

[17] Hess, B.; Kutzner, C.; van der Spoel, D.; Lindahl, E. *J Chem. Theory Comput.* 2008, *4* (3), 435-447.

[18] Marrink, S. J.; Risselada, H. J.; Yefimov, S.; Tieleman, D. P.; Vries, A. H. *J. Phys. Chem. B* 2007, *111* (27), 7812-7824.

[19] Hess, B.; Bekker, H.; Berendsen, H. J. C.; Fraaije, J. G. E. M. *J. Comput. Chem.* 1997, *18* (12), 1463-1472.

[20] Berendsen, H. J. C.; Postma, J. P. M.; van Gunsteren, W. F.; DiNola, A.; Haak, J. R. *The Journal of Chemical Physics* 1984, *81* (8), 3684.

[21] Goihman-Yahr, M. *Clin. Dermatol.* 1996, *14* (2), 153-160.

[22] Kupai, K.; Szucs, G.; Cseh, S.; Hajdu, I.; Csonka, C.; Csont, T.; Ferdinandy, P. *J. Pharmacol. Toxicol. Methods* 2010, *61* (2), 205-209.

[23] Nishimori, Y.; Edwards, C.; Pearse, A.; Matsumoto, K.; Kawai, M.; Marks, R. *J. Investig. Dermatol.* 2001, *117*, 1458-63.

[24] Fisher, G. J.; Datta, S. C.; Talwar, H. r. S.; Wang, Z.-Q.; Varani, J.; Kang, S.; Voorhees, J. J. *Nature* 1996, *379* (6563), 335-339.

[25] Chung, L.; Dinakarpandian, D.; Yoshida, N.; Lauer-Fields, J. L.; Fields, G. B.; Visse, R.; Nagase, H. *EMBO J.* 2004, *23* (15), 3020-3030.

[26] (a) Oh, E. J.; Park, K.; Kim, K. S.; Kim, J.; Yang, J.-A.; Kong, J.-H.; Lee, M. Y.; Hoffman, A. S.; Hahn, S. K. *J. Control. Release* 2010, *141* (1), 2-12; (b) Li, Y.; Rodrigues, J.; Tomas, H. *Chem. Soc. Rev.* 2012, *41* (6), 2193-2221; (c) Walpita, D.; Hay, E. *Nat Rev Mol Cell Biol* 2002, *3* (2), 137-141; (d) Ropponen, K.; Tammi, M.; Parkkinen, J.; Eskelinen, M.; Tammi, R.; Lipponen, P.; Ågren, U.; Alhava, E.; Kosma, V.-M. *Cancer Res.* 1998, *58* (2), 342-347.

[27] (a) Tsukahara, K.; Nakagawa, H.; Moriwaki, S.; Takema, Y.; Fujimura, T.; Imokawa, G. *Int. J. Dermatol.* 2006, *45* (4), 460-468; (b) Cauchard, J.-H.; Berton, A.; Godeau, G.; Hornebeck, W.; Bellon, G. *Biochem. Pharmacol.* 2004, *67* (11), 2013-2022.

[28] Dulińska-Molak, I.; Pasikowska, M.; Pogoda, K.; Lewandowska, M.; Eris, I.; Lekka, M. *Int. J.Pept. Res.Ther.* 2014, *20* (1), 77-85.

[29] (a) Solis, M. A.; Chen, Y.-H.; Wong, T. Y.; Bittencourt, V. Z.; Lin, Y.-C.; Huang, L. L. H. *Biochemistry Research International* 2012, *2012*, 11; (b) Papakonstantinou, E.; Roth, M.; Karakiulakis, G. *Dermato-endocrinology* 2012, *4* (3), 253-258.

[30] (a) Daga, R. R.; Lee, K.-G.; Bratman, S.; Salas-Pino, S.; Chang, F. *Nat. Cell Biol.* 2006, *8* (10), 1108-1113; (b) Karsenti, E.; Nedelec, F.; Surrey, T. *Nat Cell Biol* 2006, *8* (11), 1204-1211.

[31] Rodriguez, O. C.; Schaefer, A. W.; Mandato, C. A.; Forscher, P.; Bement, W. M.; Waterman-Storer, C. M. *Nat. Cell. Biol.* 2003, *5* (7), 599-609.

[32] Hotulainen, P.; Lappalainen, P. *J. Cell Biol.* 2006, *173* (3), 383-394.

Received: March 20, 2015 **Revised: April 16, 2015** **Accepted: April 20, 2015**